Well pad-level geospatial differences in the carbon footprint and direct land use change impacts of natural gas extraction

Supplemental Information

Amir Sharafi,[a,b] Marie-Odile P. Fortier[b]*

a. Environmental Systems Graduate Group, University of California, Merced, 5200 North Lake Road, Merced, CA 95343, USA.
b. Department of Civil and Environmental Engineering and Construction, University of Nevada, Las Vegas, 4505 South Maryland Parkway, Las Vegas, NV 89154, USA.

*Corresponding author, marie-odile.fortier@unlv.edu

List of Tables:

List of Figures:

Table S1: Comparison of this study with other selected natural gas life cycle assessments that include direct land use change considerations.

Feature	This study	NETL (2019) [1]	Jordaan et al. (2019) and Yeh et al. (2010) [2, 3]
Scale of scenarios	Well pad	Basin or play	Production site, then generalized to state or province
Number of scenarios	12,564	14 basin scenarios informed by individual well sites	400 [4]
Future conditions modeled	Permanent land use change (no reclamation)	Both permanent and temporary land use change	Reclamation occurs
Direct land use change impacts included	• Loss of biomass carbon • Loss of soil organic carbon • Loss of net primary productivity • Albedo change	• Loss of biomass carbon • Loss of soil organic carbon • Change in annual soil carbon uptake	• Loss of biomass carbon • Loss of soil organic carbon • Loss of net primary productivity ("foregone sequestration")
Determination of well pad areas	Machine learning methods	Citing industry averages	Filtered aerial imagery and image analysis
Well pad areas modeled	400-38,200 m^2/pad measured in GIS from delineated areas	1,000 - 20,200 m^2/pad	0.001-1 m^2/MWh
Identification of land cover & land characteristics	National Land Cover Dataset & Level III Ecoregions	Grassland and forest	High, mid, and low land disturbance intensity
Sources of data for venting and flaring impacts, and gas used at the site	Direct report by the New Mexico's Energy Minerals and Natural Resources Department, [5], and leakage rate per year was applied for the remaining lifetime years of wells [1]	Direct measurement and reports along with the literature	Venting at extraction is not considered
Determination of natural gas production	For wells between 25 to 50 years old, predicted production is equal to the area under the decline line between the average of the last 4 years' production and 180 Mcf for the 50th year of the well. 180 Mcf per year is the economic justification for continuing production [6], although, for wells under 25 years old, a decline exponential curve was applied instead of a decline line. Decline rate was obtained from historical data of older gas wells.	GHGRP Data and Drilling Info were used to cover information for historical data, and approaches for gathering future data were not mentioned.	Estimated Ultimate Recovery (EUR) was employed by applying a decline curve analysis for estimating the well's producing lifetime
Determination of well pad lifetimes	Calculated by well as described in Section 2.2 of the manuscript.	Estimated ultimate recovery (EUR) was used to determine the productive life of wells. DI Desktop tool was employed to estimate EUR.	EUR was used to estimate the lifespan of gas wells, which the study determined to be 25 years old.

** If the average lifetime of plugged-on wells is taken into effect, it drops to 45 years old, but this does not apply because technological advances were not considered in the approach.

Table S2: Life cycle assessment model parameters and their data sources.

Parameter name	Parameter description	Units	Data sources
New Mexico well database-informed parameter values:			
Vertical depth	Maximum vertical depth of the well reported	m	EMNRD [5]
Horizontal length	Maximum length of the horizontal part of the well	m	EMNRD
Gas production	Total annual and monthly gas production per well	Mcf/well	EMNRD
Oil production	Total oil production per well	BBL/well	EMNRD
Vented gas	Total amount of vented gas per well	Mcf/well	EMNRD
Casing type	Casing structure type identified from shape reported for each well (complex, moderate, and simple well design casing structures)		EMNRD; [7]
Cement	Amount of cement used in the casing for each section of the well	sacks	EMNRD
Steel	Amount of steel used in the casing for each section of the well	lb/ft	EMNRD
Spud year	Operational lifespan of the well	year	EMNRD
Distance	Road distance from a well pad to the named owner's nearest warehouse	km	EMNRD; GIS
Satellite/GIS dataset-informed parameter values:			
Aboveground biomass C	Carbon in the aboveground biomass on the original land	$t\ C\ ha^{-1}$	[8] & [9]
Belowground biomass C	Carbon in the belowground biomass on the original land	$t\ C\ ha^{-1}$	[8] & [9, 10]
Soil organic carbon (SOC)	SOC content of the original land	$g\ C\ m^{-2}$	gSSURGO [10, 11]
NPP	Net primary productivity under the original land conditions	$g\ C\ m^{-2}\ year^{-1}$	Landsat 8 [12, 13]
Surface albedo	Sunlight reflecting capability of the surface at a given location	Unitless	Landsat 8
Slope	250-m resolution slope raster file for the contiguous 48 states	Percent slope	USGS Seamless, Argonne National Laboratory

EMNRD=New Mexico's Energy Minerals and Natural Resources Department, Mcf=tousand cubic feet, BBL=barrel, t=metric tonne, ha=hectare.

Table S3: General construction parameters and their data sources.

Parameter name	Value	Units	Sources of modeled data
Bulldozer mass	22,000	kg/machine	[14]
Bulldozer diesel consumption rate	37	L/hour	[15]
Regular cleaning time	0.00098	h/m^2	[14]
Excavator mass	18,000	kg/machine	Estimated from popular Caterpillar model size
Excavator diesel consumption rate	28	L/hour	Estimated from popular Caterpillar model size
Motor grader mass	13,000	kg/machine	Estimated from popular Caterpillar model size
Motor grader diesel consumption rate	15	L/hour	Estimated from popular Caterpillar model size
Vibratory compactor mass	9000	kg/machine	Estimated from popular Caterpillar model size
Vibratory compactor diesel consumption rate	12	L/hour	Estimated from popular Caterpillar model size
Compactor operational time	627	m^2/hour	
Gravel density	1680	kg/m^3	
Concrete pad thickness (selected till can tolerate high pressure)	0.2032	m	YouTube videos
Gravel thickness	0.1524	m	YouTube videos
Cement sacks for casing	25	kg/sack	
Dumping distance for mud and vegetation waste	25	km	
Reinforcement percentage for steel in the concrete pad	3	%	
Productivity of the excavator in digging soil	60	m^3/hour	
Rig equipment mass (overall), for drill, pumpjack, and power generator	82,500	kg	
Operation equipment mass (overall), for lift system, mechanical pumps, storage tanks, small to medium-scale compressors	42,800	kg	
Fuel estimation for drilling	variable	L	[7, 16]
Fuel for hydraulic fracturing	variable	L	[7, 16]
Sands (gravel) in fracture liquid	0.3	kg/L	

Table S4: Life cycle inventories from databases used in this study

Life cycle inventory or data point name	Source	Impact units	Applications in this study
Concrete block | market for concrete block | APOS, U	Ecoinvent 3	kg CO2eq/ kg concrete	Impact of producing concrete
Steel, low-alloyed | steel production, converter, low-alloyed | APOS, U	Ecoinvent 3	kg CO2eq/ kg steel	Impact of producing steel
Provision of gravel	[17]	kg CO2eq/ t gravel	Impact of producing gravel
Transport, single-unit truck, short-haul, diesel-powered/ tkm/ RNA	USLCI	kg CO2eq/ t x km	Transportation with SU track
Using Diesel	EPA - Emission Factors for Greenhouse Gas Inventories	kg CO2eq/ gallon diesel	Impact of burning diesel
Using natural gas	EPA - Emission Factors for Greenhouse Gas Inventories	kg CO2eq/ scf natural gas	Impact of burning natural gas
Diesel, low-sulfur | market group for | APOS, S	Ecoinvent 3	kg CO2eq/kg diesel	Impact of producing diesel fuel

GHG=greenhouse gas, APOS=at point of substitution, S=system, RoW=rest of world, RNA=Rest of North America, U=unit

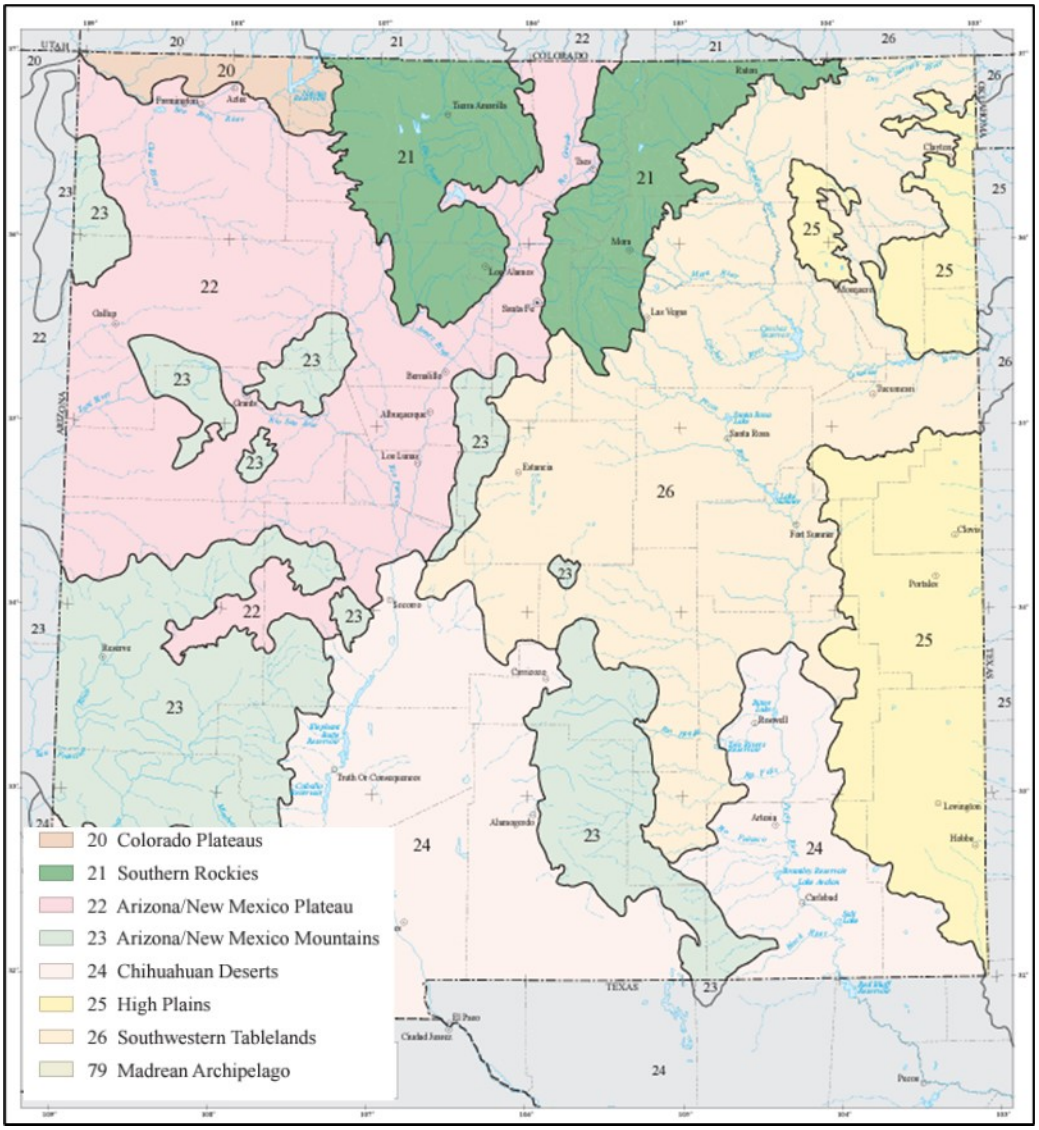

Figure S1: Level III ecoregion map representing distinct ecological areas in New Mexico [18].

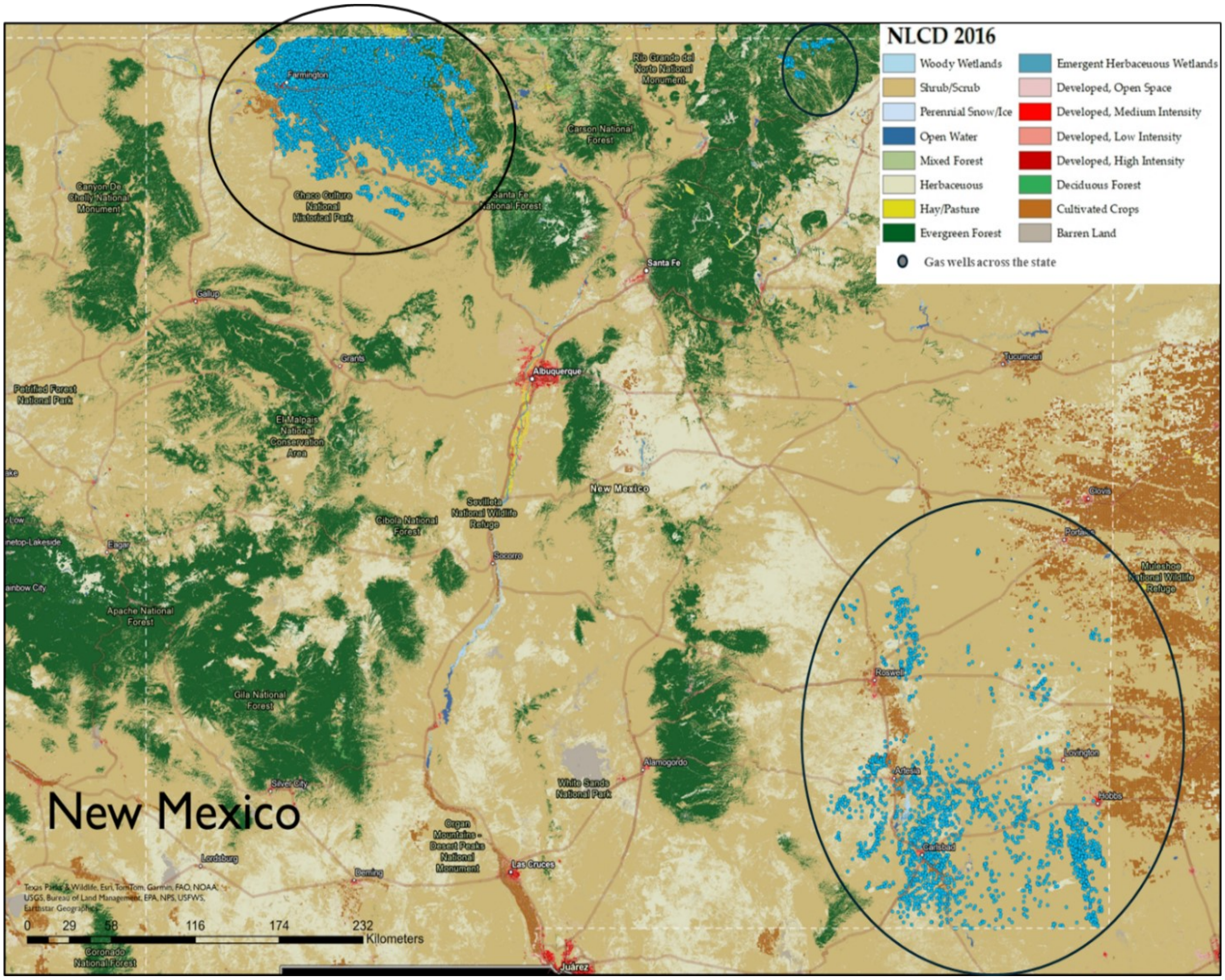

Figure S2: Land cover diversity in New Mexico [8] and distribution of gas wells across the state (blue dots).

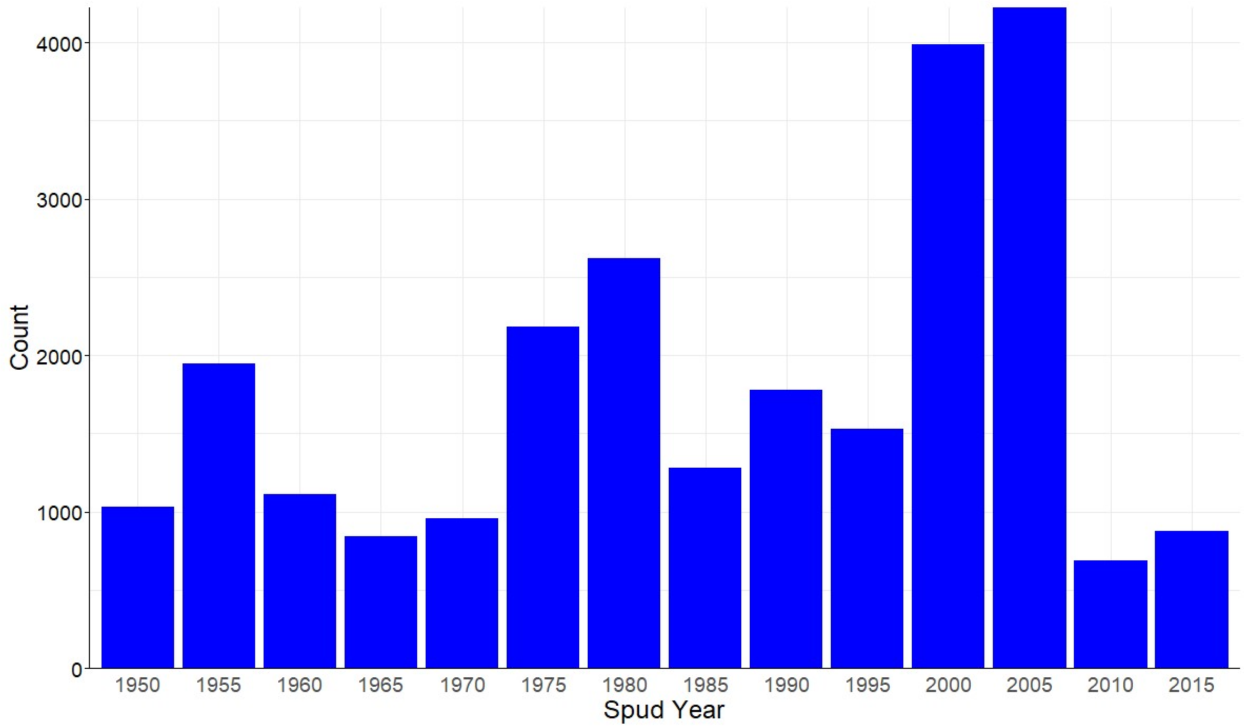

Figure S3: The distribution of operational natural gas-producing wells in New Mexico, categorized by five-year intervals of their construction years from 1950 to 2020.

.

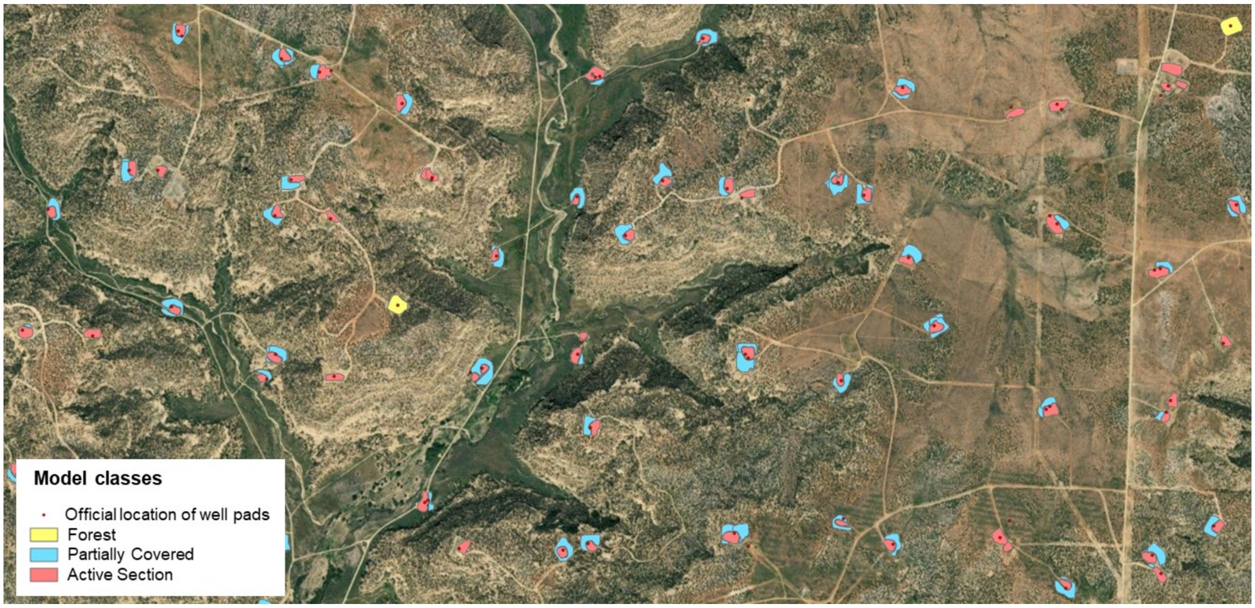

Figure S4: Representative example of the resulting segmentation quality for three classes: forest, partially covered, and active section, in comparison with the official point locations of wells reported by the state.

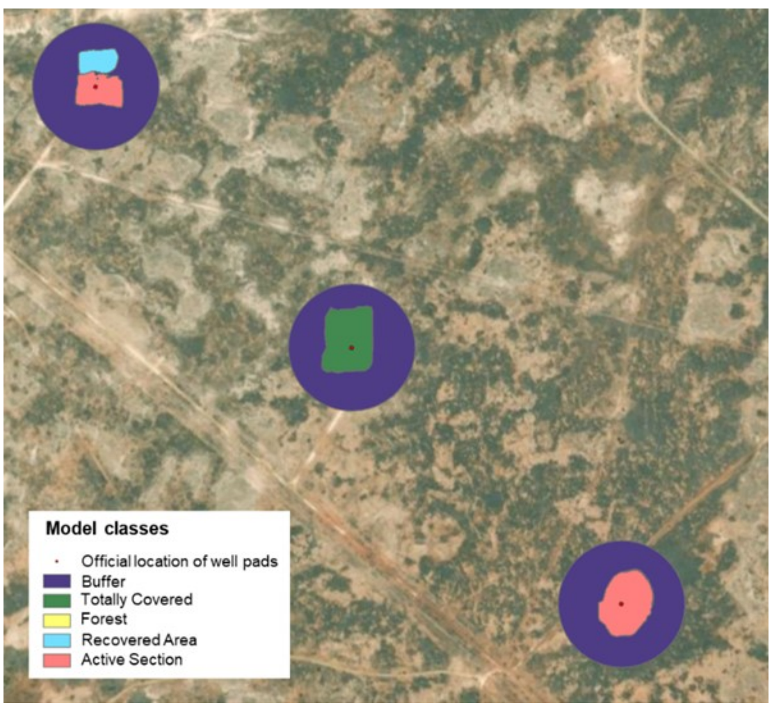

Figure S5: Representative closer view of the various classes with 100-m radius circular buffers and the reported point locations of the wells.

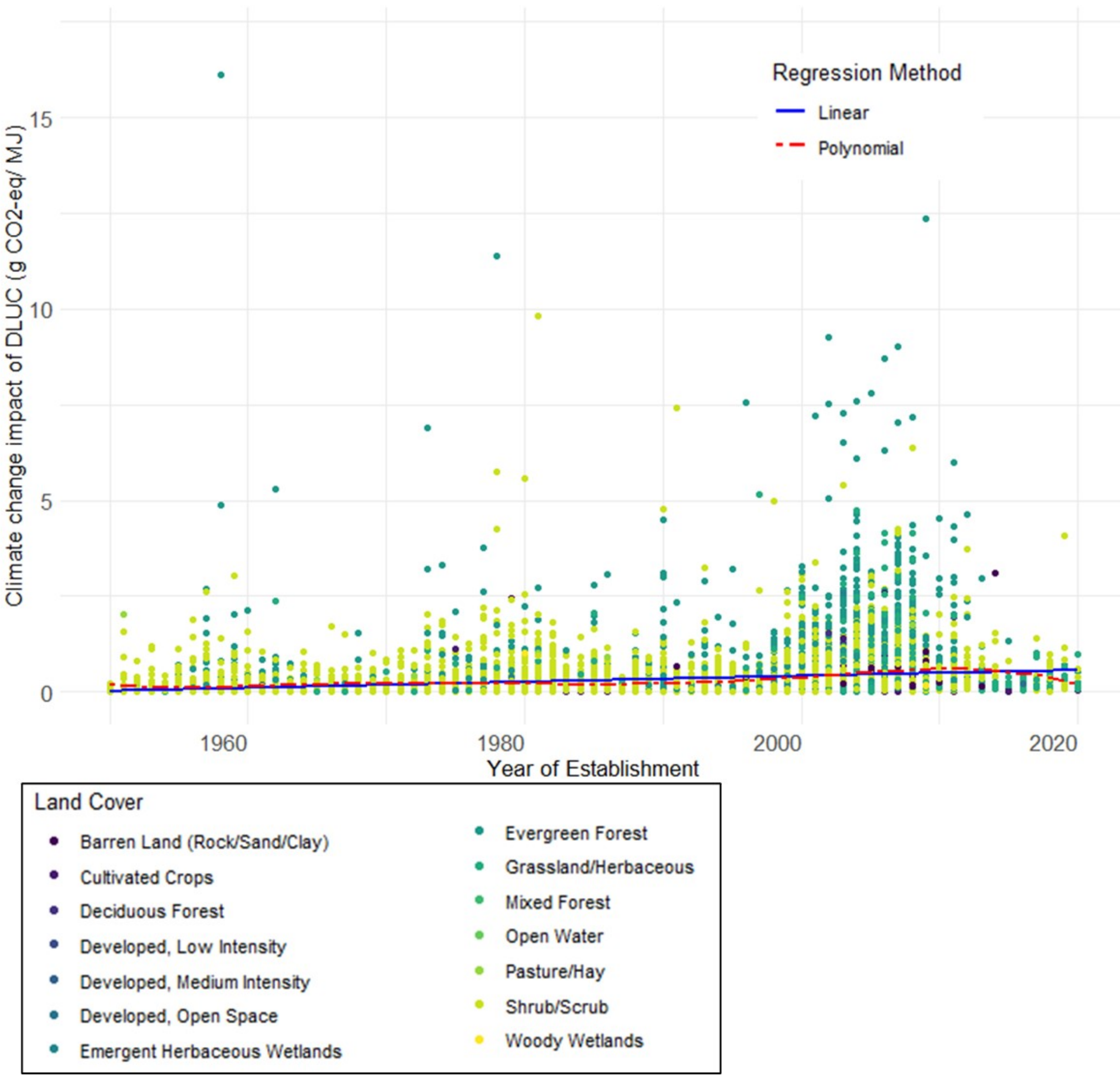

Figure S6: Distribution of the climate change impacts of gas wells by spud year and land cover type.

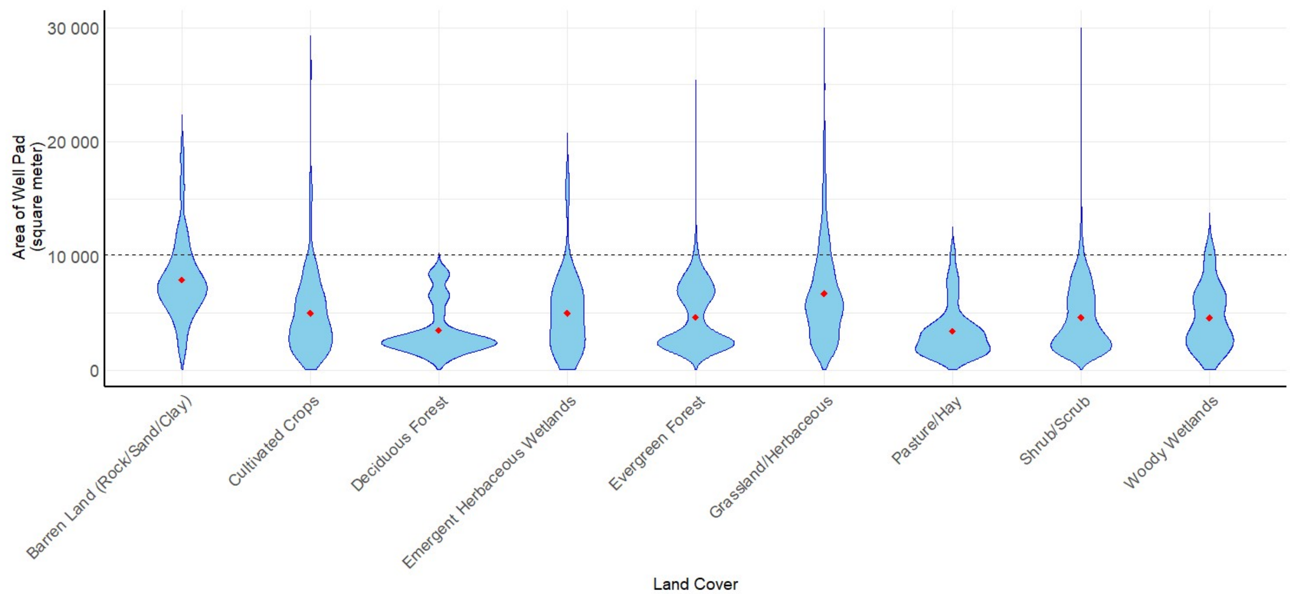

Figure S7: Well pad areas detected by machine learning techniques by land cover type, compared against the NETL (2019) report's average well pad area for conventional wells. The Black dashed line is the average area of well pads reported by NETL.

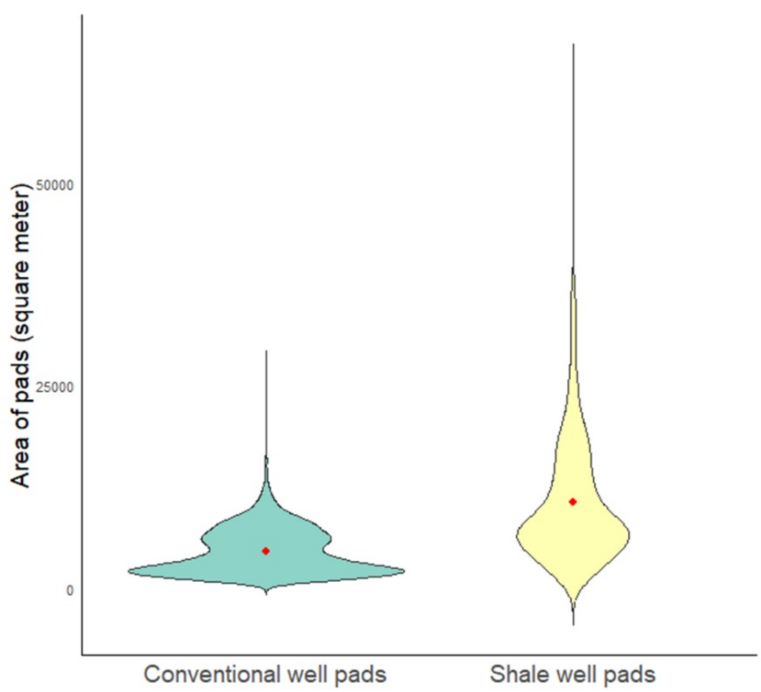

Figure S8: Areas of gas well pads in New Mexico by method of extraction, conventional and shale gas.

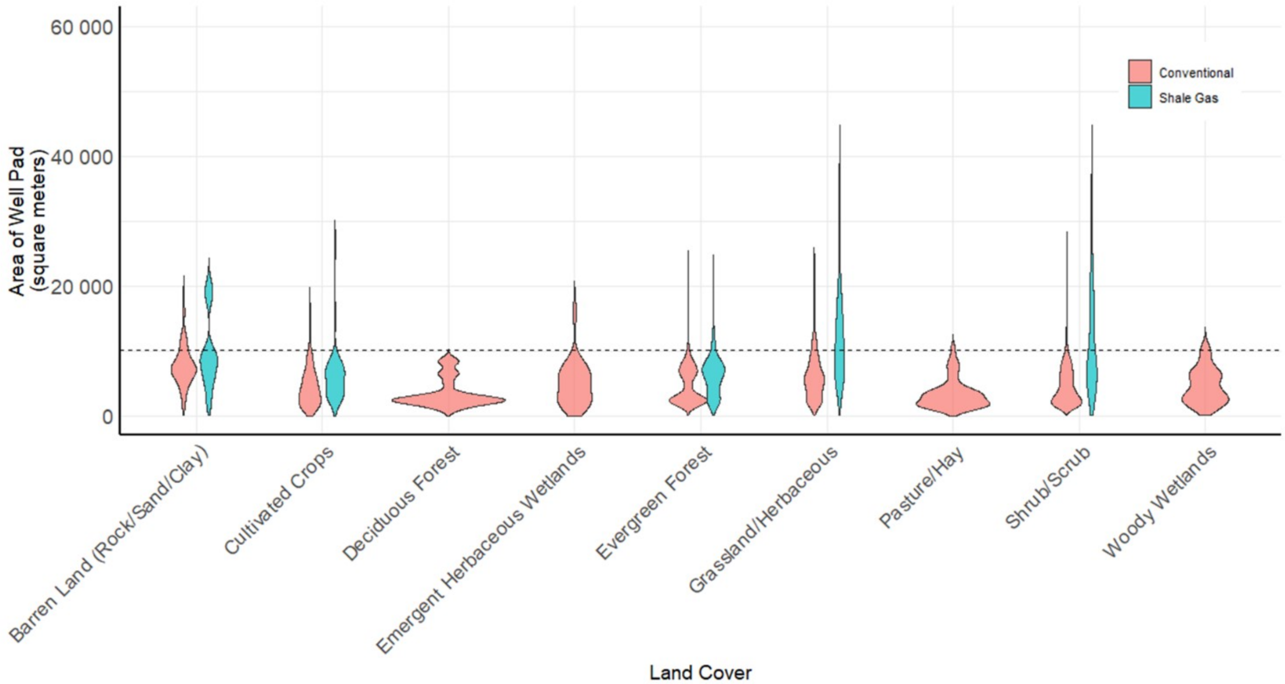

Figure S9: Well pad areas by type of extraction and by land cover type. The black dashed line is the average area of well pads reported by NETL.

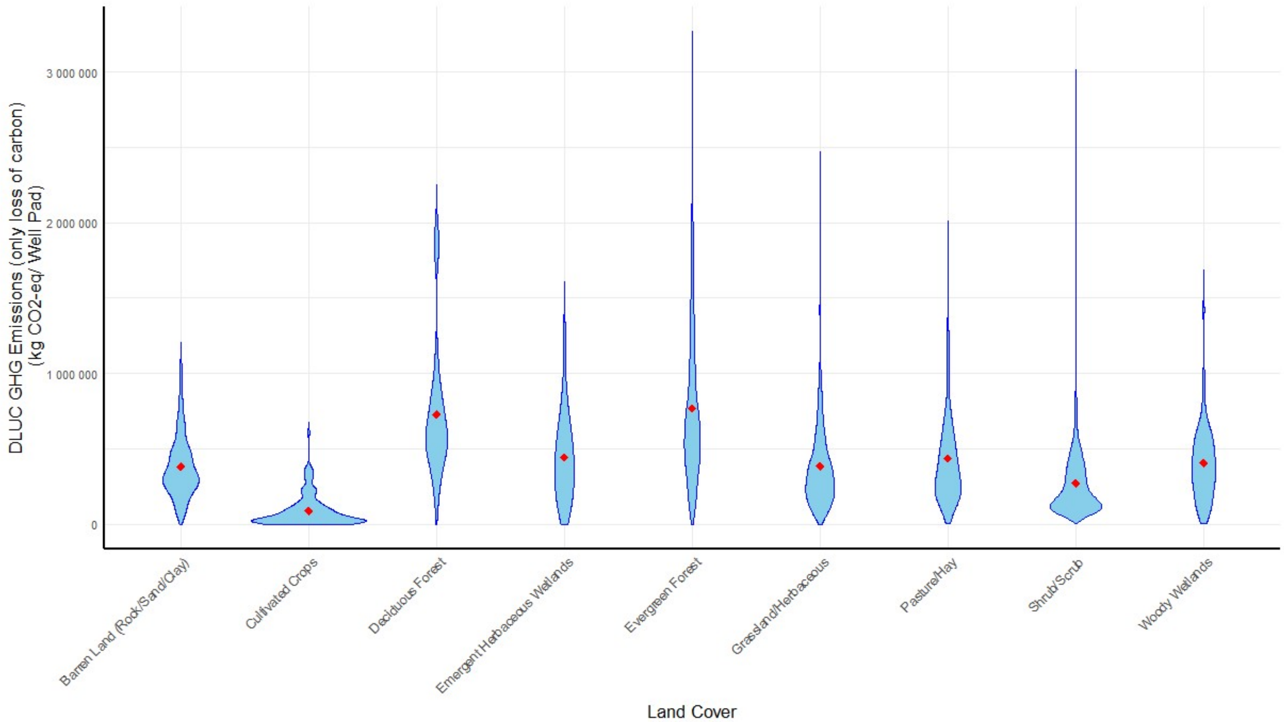

Figure S10: Carbon-related direct land use change (DLUC) effects per well pad, excluding surface albedo change, categorized by land cover. Developed types of land cover are excluded from this figure due to their low numbers.

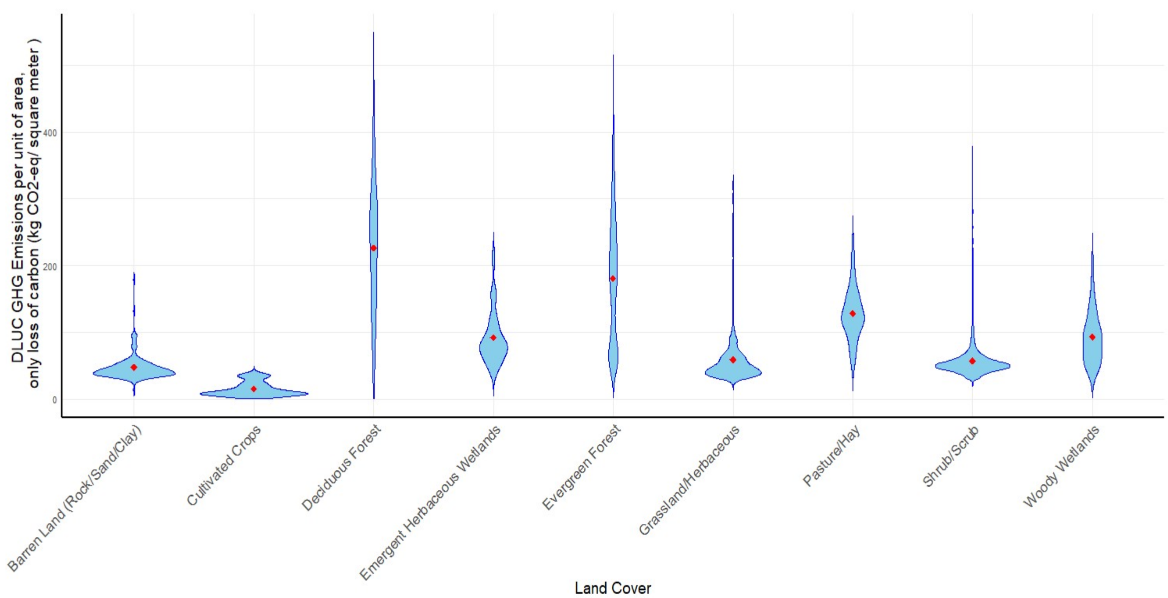

Figure S11: Carbon loss per square meter due to direct land use change (DLUC) effects classified by type of land cover (surface albedo change impacts excluded).

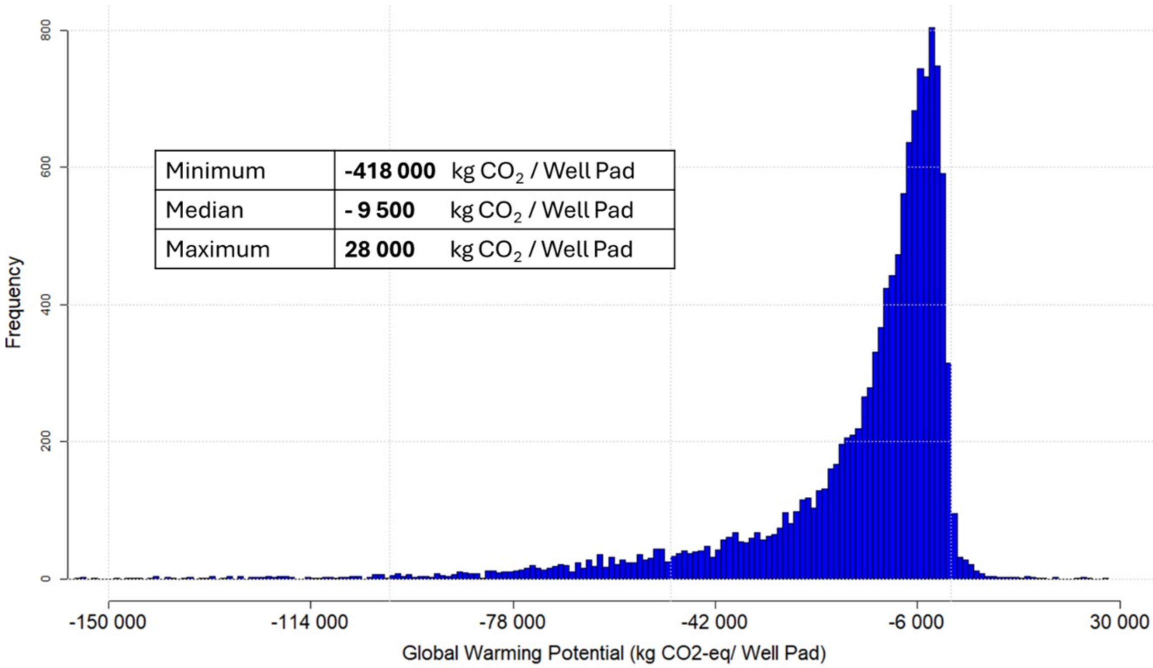

Figure S12: Distribution of surface albedo change impacts in units of kg CO_2eq per well pad.

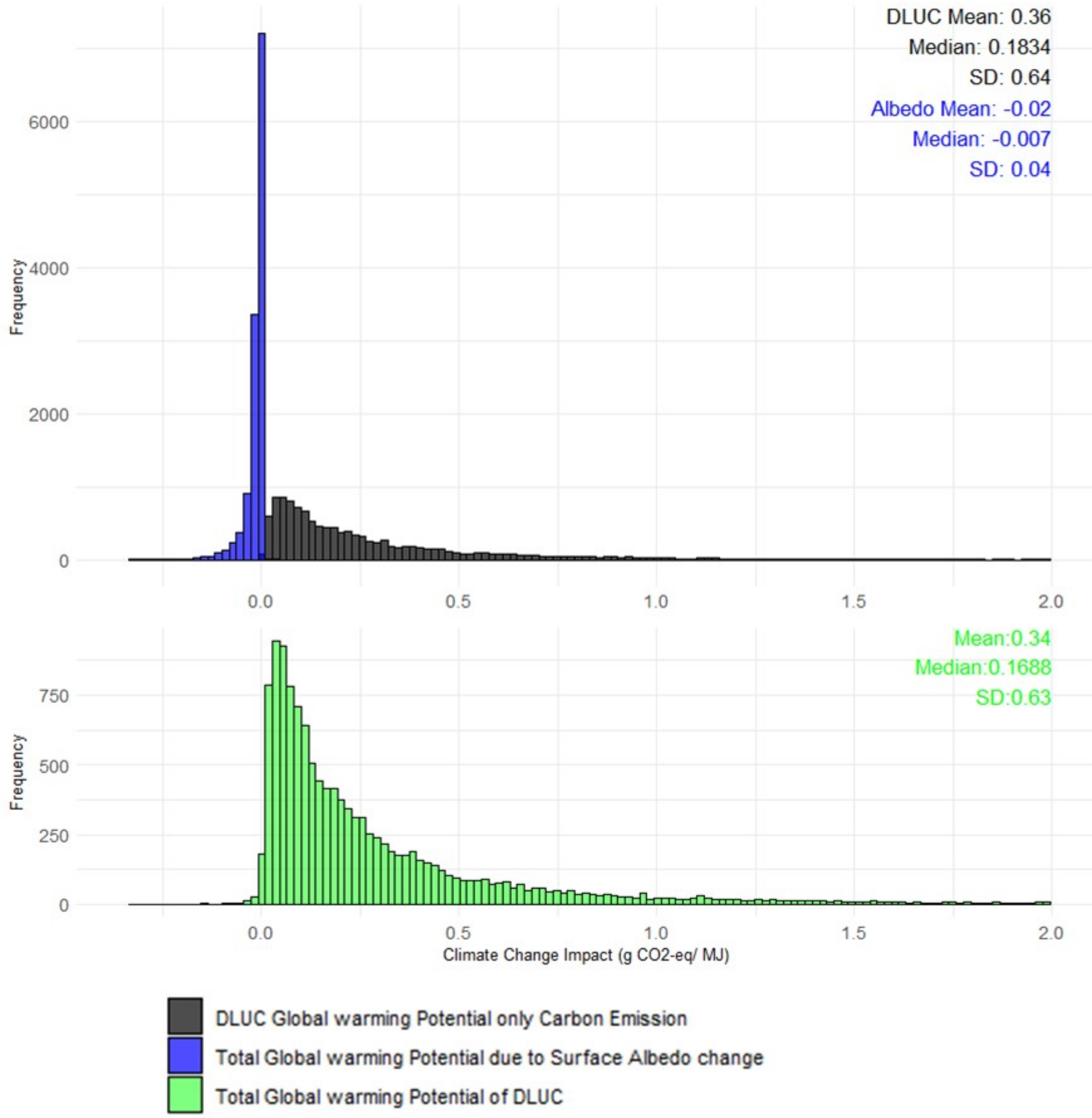

Figure S13: Albedo change impacts relative to only carbon-related DLUC impacts (top histograms) and the total climate change impact from these combined effects (bottom histogram).

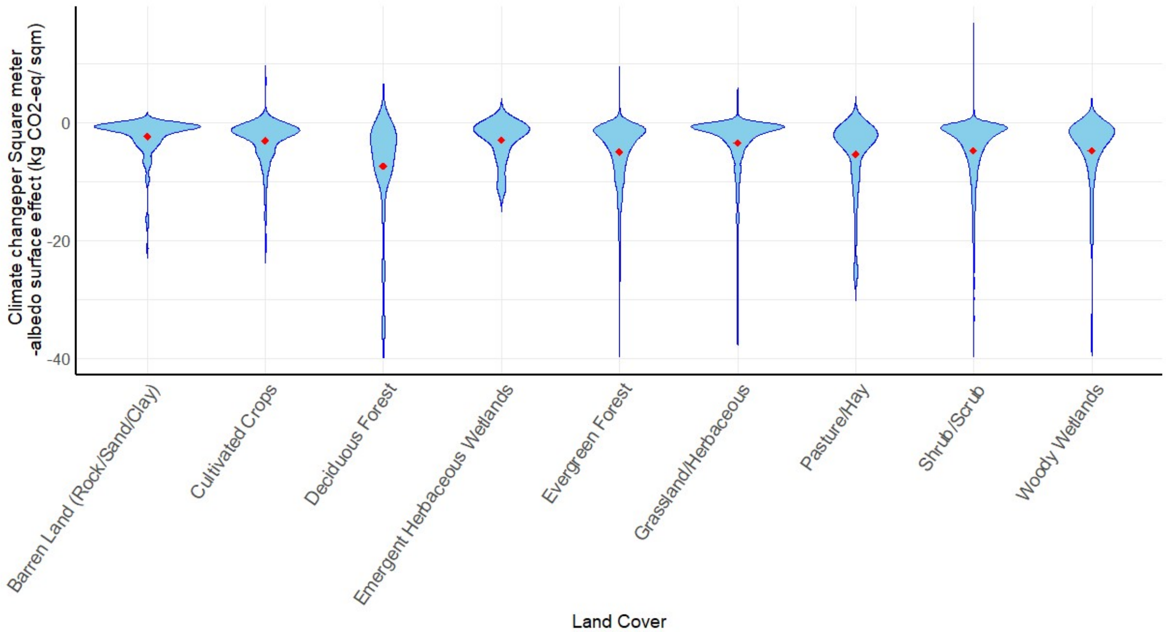

Figure S14: Surface albedo change impact of well pads in kg CO_2eq/m^2 by land cover type.

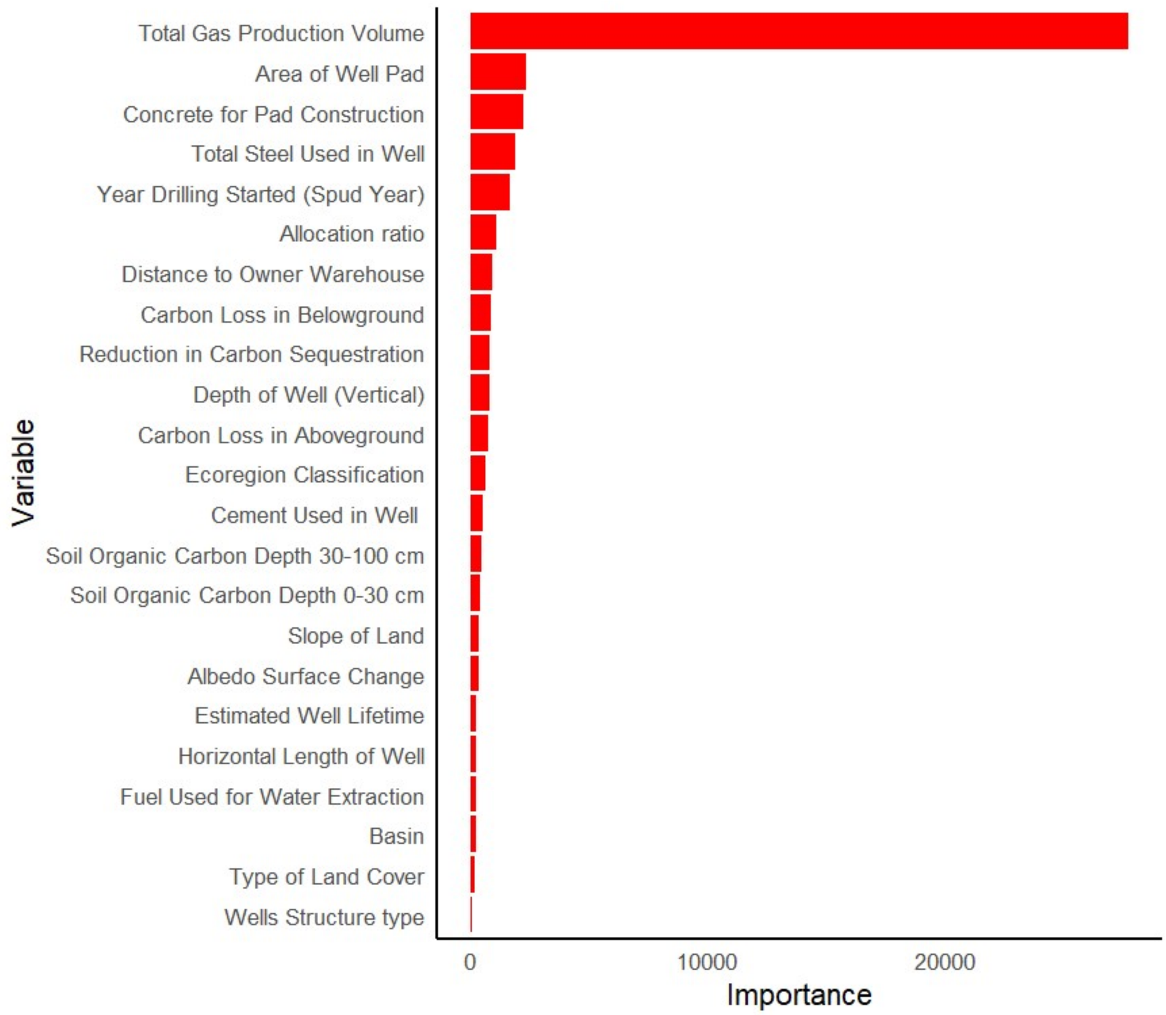

Figure S15: Random forest results identifying the most influential variable to be the total gas production in the entire lifespan.

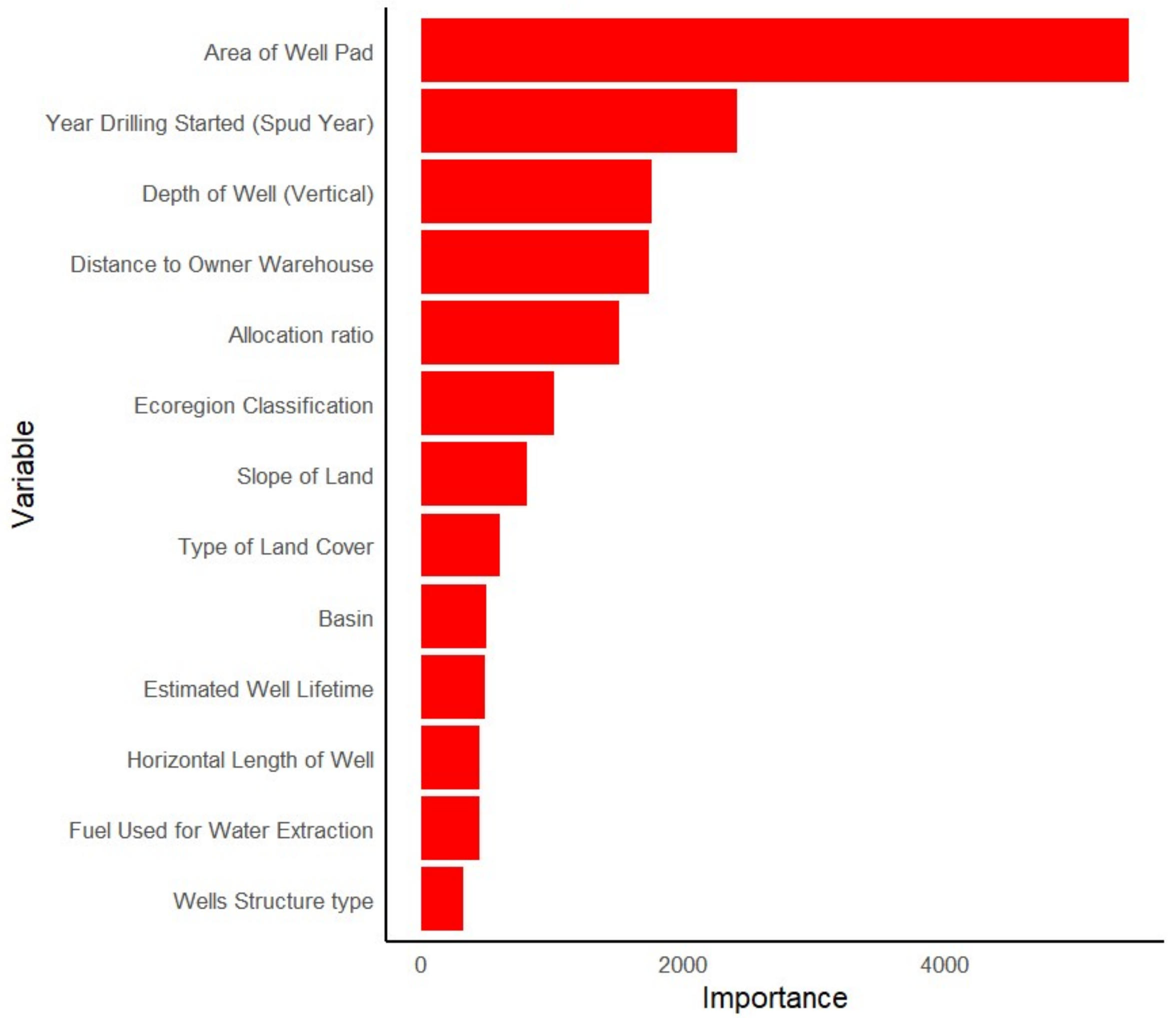

Figure S16: The importance of input parameters after eliminating variables with complex and partial connections.

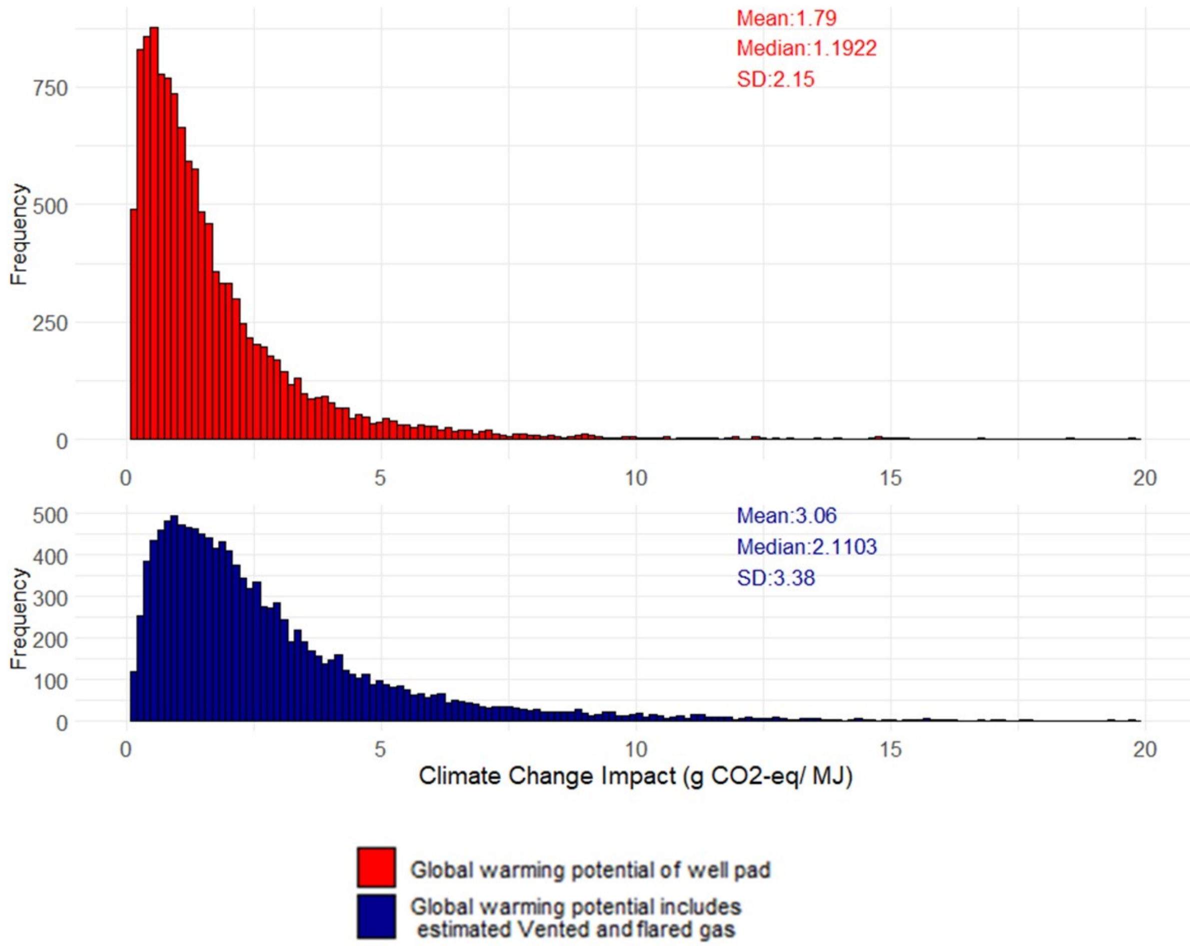

Figure S17: Total global warming potential of establishing a well pad and drilling the wells (top) and the total climate change impact, including estimated vented and flared gas (bottom).

.

S1. Assessing the global warming potential of surface albedo change

The Global Warming Potential (GWP) method converts the impact of various GHG emissions or alterations in non-GHG climate change drivers to their relative contribution to climate change in commons units of an equivalent amount of CO_2 emitted over a specified time horizon. Similarly, to incorporate albedo change into the net climate change impacts of natural gas well pads, the difference in surface albedo for the well pad area during its lifetime was transformed into equivalent carbon dioxide units for each well pad area. Global warming potential (GWP) associated with the changes in surface albedo at a specific location can be computed by time-integrating the global radiative forcing due to albedo change normalized by the radiative forcing of CO_2 over the same time horizon, as shown in Equation 1 [19].

$$GWP_w(TH) = \frac{A_w \int_0^{TH} \Delta RF_{\alpha}^{Global}(t)dt}{A_E \int_0^{TH} \Delta RF_{CO_2}(t)dt} \tag{1}$$

A_T is total area of well pads in recent years (m^2), A_E is Earth's surface area (5.1×10^{14} m^2). The global radiative forcing (ΔRF) is calculated through Equation 2 to equate the effect of changes in natural factors on climate change impact with $CO_{2\text{-eq}}$ emissions [19, 20].

$$\int_0^{TH} \Delta RF_{\alpha}^{Global}(t)dt = \int_0^{TH} -R_{TOA,ann}K_{T,ann}T_a\Delta\alpha_{s,ann}y_{\alpha}(t)dt \tag{2}$$

Where R_{TOA} is the portion of solar radiation that reaches the top of Earth's atmosphere every day; it is the product of the solar constant (1362 $\frac{W}{m^2}$), the latitude of the location, and the day of the year [20]. K_T, the clearness index, is the amount of solar insolation at the Earth's surface, measured by NASA since 1984, and the transmittance factor is T_a [20]. The ratio of the reflected radiation from the surface is called surface albedo, which is measured on a scale of zero to one, and it can be determined through remote sensing methods.

To determine surface albedo in this study, remote sensing techniques based on Landsat 8 Level 2 satellite imagery were used. Level 2 data refers to further processing and correction of calibrated data (level 1) [21], which became available shortly after the launch of Landsat 8 in 2013. The difference in the fraction of shortwave radiation reflected from the surface over time is called surface albedo change ($\Delta\alpha_s$), which is measured on a scale of zero to one. The albedo decay function $y_{\alpha}(t)$ ranges from zero to one; sincethe whole-time horizon was under study, it was set 1 in this study. Because the study investigates global warming impacts on a 100-year time horizon, *TH* is 100 in this equation. The radiative forcing of CO_2 can be defined through Equation (3) [19, 22].

$$\int_0^{TH} \Delta RF_{CO_2}(t)dt = \int_0^{TH} k_{CO_2} y_{CO_2}(t)dt \tag{3}$$

Like $y_\alpha(t)$, $y_{CO_2}(t)$ is a decay function, but for CO_2. The radiative efficiency of CO_2 per kg of emission (k_{CO_2}) is derived from products of the molecular weight of CO_2 and air, the radiative efficiency for an increase of 1 ppm in the concentration of CO_2, and the mass of the atmosphere [19]. Consequently, the greenhouse gas emissions equivalent of shortwave forcing in kg $CO_{2\text{-eq}}/m^2$ can be expressed as:

$$GWP_w(100) = \frac{A_w \times \sum_0^{100} \Delta RF_\alpha(t)}{A_E \times k_{CO_2} \times \sum_0^{100} y_{CO_2}(t)} \tag{4}$$

With this approach, $GWP_w(100)$ represents the effect of albedo change for 100 years; therefore, the results can be compared with the other CO_2eq inventory of the LCA, which uses a 100-year time horizon. However, to calculate the impact of surface albedo change for less than 100 years with only the conditions before and after conversion, assuming that only one change happened in the surface albedo of the area and that the albedo of the surface remains relatively the same prior to conversion and then also once the change occurs, the following equation can be used to determine the global warming potential of the change in albedo (Equation 5):

$$GWP_w(T) = \frac{A_w \times - R_{TOA,ann} K_{T,ann} T_a(\alpha_{current} - \alpha_{pre-change})}{A_E \times k_{CO_2} \times 100} \tag{5}$$

In this equation, the surface condition of pads was assumed to stay constant for over 100 years after establishment, which is equal to the average condition of 2014-2022. Due to a lack of high-quality images for all wells, the above assumption was taken to calculate the albedo of the well gas pads. Therefore, the most accurate results belong to pads aged 40 to 60 years old, while results of pads with establishment years near both ends may have overestimated and underestimated results.

References

1. Jeffrey Logan, G.H., Jordan Macknick, Elizabeth Paranhos, Ken Carlson and William Boyd, *Natural Gas and the Transformation of the U.S. Energy Sector: Electricity*. 2012.
2. Jordaan, S., *Wells to Wire*. 2021: Springer Cham. 115.
3. Yeh, S., et al., *Land Use Greenhouse Gas Emissions from Conventional Oil Production and Oil Sands.* Environmental Science & Technology, 2010. **44**(22): p. 8766-8772.
4. Patzek, T.W., F. Male, and M. Marder, *Gas production in the Barnett Shale obeys a simple scaling theory.* Proceedings of the National Academy of Sciences, 2013. **110**(49): p. 19731-19736.
5. New Mexico Department of Energy, M., and Natural Resources. *OCD GIS and Maps*. 2023; Available from: https://www.emnrd.nm.gov/ocd/ocd-gis-and-maps/#:~:text=Brine%20Wells%20Map&text=There%20are%20a%20total%20of,with%20oil%20and%20gas%20development.
6. Weber, J.G., et al., *Identifying the end: Minimum production thresholds for natural gas wells.* Resources Policy, 2021. **74**: p. 102404.
7. Brandt, A.R., *Embodied Energy and GHG Emissions from Material Use in Conventional and Unconventional Oil and Gas Operations.* Environmental Science & Technology, 2015. **49**(21): p. 13059-13066.
8. Center, E.R.O.a.S.E. *National Land Cover Database* 2001; Available from: https://www.usgs.gov/centers/eros/science/national-land-cover-database.
9. Alvarez, E., et al., *Tree above-ground biomass allometries for carbon stocks estimation in the natural forests of Colombia.* Forest Ecology and Management, 2012. **267**: p. 297-308.
10. Spawn, S.A., et al., *Harmonized global maps of above and belowground biomass carbon density in the year 2010.* Scientific Data, 2020. **7**(1): p. 112.
11. U.S. Department of Agriculture, N.R.C.S., *Gridded Soil Survey Geographic (gSSURGO) Database.* 2023.
12. Robinson, N.P., et al., *Terrestrial primary production for the conterminous United States derived from Landsat 30 m and MODIS 250 m.* Remote Sensing in Ecology and Conservation, 2018. **4**(3): p. 264-280.
13. Group., N.T.S., *Landsat Productivity.*, U.o.M. Retrieved, Editor. 2019.
14. *WHAT EQUIPMENT IS USED FOR CLEARING LAND?* 2023; Available from: https://cospringsexcavation.com/what-equipment-is-used-for-clearing-land/.
15. *Average Bulldozer Fuel Consumption (How Much Fuel Does A Dozer Burn?)*. 2023; Available from: https://eduautos.com/average-bulldozer-fuel-consumption-how-much-fuel-does-a-dozer-burn/.
16. El-Houjeiri, H.M., A.R. Brandt, and J.E. Duffy, *Open-Source LCA Tool for Estimating Greenhouse Gas Emissions from Crude Oil Production Using Field Characteristics.* Environmental Science & Technology, 2013. **47**(11): p. 5998-6006.
17. de Bortoli, A., *Understanding the environmental impacts of virgin aggregates: Critical literature review and primary comprehensive life cycle assessments.* Journal of Cleaner Production, 2023. **415**: p. 137629.
18. Omernik, J.M. and G.E. Griffith, *Ecoregions of the Conterminous United States: Evolution of a Hierarchical Spatial Framework.* Environmental Management, 2014. **54**(6): p. 1249-1266.
19. Bright, R.M., F. Cherubini, and A.H. Strømman, *Climate impacts of bioenergy: Inclusion of carbon cycle and albedo dynamics in life cycle impact assessment.* Environmental Impact Assessment Review, 2012. **37**: p. 2-11.
20. Fortier, M.-O.P., et al., *Determination of the life cycle climate change impacts of land use and albedo change in algal biofuel production.* Algal Research, 2017. **28**: p. 270-281.
21. Robinson, N.P., et al., *Terrestrial primary production for the conterminous United States derived from Landsat 30 m and MODIS 250 m.* Remote Sensing in Ecology and Conservation, 2018. **4**(3): p. 264-280.
22. Bright, R.M. and M.T. Lund, *CO2-equivalence metrics for surface albedo change based on the radiative forcing concept: a critical review.* Atmos. Chem. Phys., 2021. **21**(12): p. 9887-9907.